IL NUOVO CIMENTO Vol. 31 C, N. 3 Maggio-Giugno 2008
DOI 10.1393/ncc/i2009-10312-1

External forcings and predictability in Lorenz model: An analysis *via* neural network modelling

Antonello Pasini(*)

Istituto sull' Inquinamento Atmosferico del CNR - via Salaria Km 29.300
I-00016 Monterotondo Stazione (Rome), Italy

(ricevuto il 3 Febbraio 2009; approvato il 9 Febbraio 2009; pubblicato online il 12 Marzo 2009)

Summary. — What's about predictability in future climate scenarios? At present, we have no answer to this question in realistic climate models, due to the need of a difficult and time-consuming analysis. So, in the present paper an investigation of this situation has been performed through low-dimensional models, by considering unforced and forced Lorenz systems as toy-models. By coupling dynamical and neural network analyses, some clear results are achieved: for instance, an increase of mean predictability in forced situations (which simply mimic the actual increase of anthropogenic forcings in the real system) is discovered. In particular, the application of neural network modelling to this problem supplies us with some "surplus" information and opens new prospects as far as the operational assessment of predictability is concerned.

PACS 05.45.Ac – Low-dimensional chaos.
PACS 92.70.Gt – Climate dynamics.
PACS 92.60.Ry – Climatology, climate change and variability.
PACS 07.05.Mh – Neural networks, fuzzy logic, artificial intelligence.

1. – Introduction

As well known, the classical Lorenz model [1] mimics some features of the climate system (and its atmospheric subsystem), such as their chaotic behaviours and the existence of preferred states or "regimes". Furthermore, it can be considered as the prototype of a large class of meteo-climatic toy models (see ref. [2] for the recognition of this class and the development of an extended formalism).

Even if somebody affirms that low-dimensional models lead to reconstruct just the climate of an "utopian world" (see, however, ref. [3]), anyway, as shown by Palmer [4,5], the adoption of a toy-model approach can be interesting in a "dynamical perspective" for the study of climate when the behaviour of low-dimensional dynamical systems resembles the dynamics of the real system. In this perspective, then, it is worthwhile to stress that

(*) E-mail: pasini@iia.cnr.it

distinct regions of the Lorenz attractor show different predictabilities, exactly as distinct types of weather situations are endowed with different predictability horizons. Moreover, it has been shown [6] that changes in the occurrence of the frequency of regimes can be observed in the Lorenz model if external forcings are added to the system, exactly as they were recognised in the real system when anthropogenic forcings increased.

Nevertheless, to author's knowledge, investigations about predictability in changed climate scenarios did not appear in the literature, till now. Of course, this kind of analysis should be quite difficult (and time-consuming) in realistic models but it is surely simpler in a low-dimensional model. Thus, the preliminary aim of this paper is to perform a brief dynamical analysis of unforced and forced Lorenz systems, just to evaluate if a clear change in predictability is shown in these two cases. This is done by computation of the so-called "bred-vector growth", following the application made by Evans *et al.* to the classical unforced Lorenz model [7].

Furthermore, during recent years neural network (NN) modelling has been developed for climate applications. In particular, it has been shown that this kind of data-driven modelling can be considered alternative to dynamical modelling, as in attribution studies, or complementary to it, as in a downscaling approach (see ref. [8] for a comprehensive conceptual and technical review). Sometimes, NNs have been used for emulating dynamical integrations, too (see [9] and references therein).

In this framework, it is interesting to study the NNs' capability of estimating predictability on the Lorenz attractors, both in the unforced and in the forced cases: this is the main aim of this paper. In doing so, we assess the performance of a NN in this forecast activity and discover some "surplus" information given by this NN modelling if compared with dynamical modelling.

In sect. **2** a NN tool, recently developed and here adopted for predictability estimation on Lorenz attractors, is presented. In sect. **3** the dynamics of a generalised Lorenz system is briefly summarised. Section **4** is devoted to perform an estimation of predictability in unforced and forced situations by a dynamical method. In sect. **5** alternative estimations of predictability are obtained by a NN model. Finally, brief conclusions are drawn and prospects of further studies are envisaged in the last section.

2. – The NN tool

A NN tool for both diagnostic characterisation and forecast activity in complex systems has been developed some years ago [10]. Since that date it has been applied to diagnostic and prognostic problems in the atmospheric boundary layer [10-13]. More recently, attribution studies in the climate system have been performed as a further application of this tool [14].

The kernel of this tool has been extensively described elsewhere (see ref. [10] for the main model and [11] for a modified version of it). Here I cite just that the NNs adopted in the present investigation are feedforward networks with one hidden layer (fig. 1) and nonlinear transfer functions (sigmoids) at the hidden and output neurons. The learning stage from data is performed by an error-backpropagation training characterised by generalised Widrow-Hoff rules (endowed with gradient descent and momentum terms) for updating the connection weights at each iteration step, as follows:

$$
\begin{aligned}
(1) \qquad W_{ij}(t+1) &= W_{ij}(t) - \eta \frac{\partial E^{\mu}}{\partial W_{ij}(t)} + m\left[W_{ij}(t) - W_{ij}(t-1)\right] \\
&= W_{ij}(t) + \eta g_i'(h_i^{\mu})(T_i^{\mu} - O_i^{\mu})V_j^{\mu} + m\left[W_{ij}(t) - W_{ij}(t-1)\right],
\end{aligned}
$$

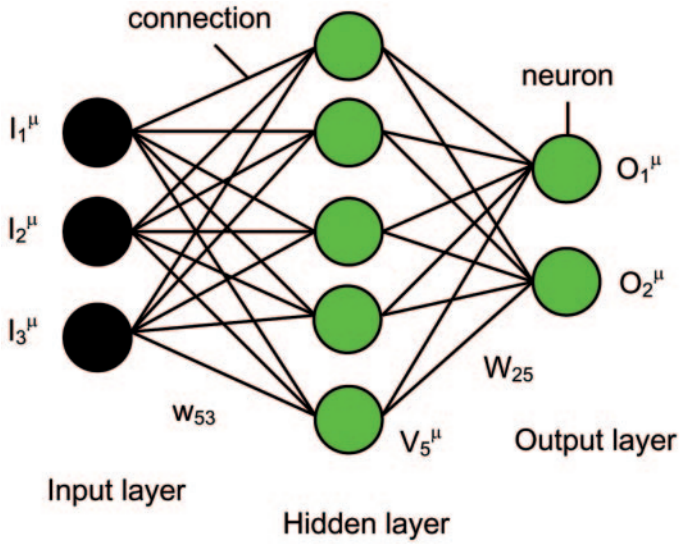

Fig. 1. – Feedforward neural network and nomenclature used in this paper.

$$
\begin{aligned}
(2) \qquad w_{jk}(t+1) &= w_{jk}(t) - \eta \frac{\partial E^\mu}{\partial w_{jk}(t)} + m\left[w_{jk}(t) - w_{jk}(t-1)\right] \\
&= w_{jk}(t) + \eta g_j'(h_j^\mu) \sum_i W_{ij} g_i'(h_i^\mu)(T_i^\mu - O_i^\mu) I_k^\mu \\
&\quad + m\left[w_{jk}(t) - w_{jk}(t-1)\right].
\end{aligned}
$$

Here, with reference to the terminology also introduced in fig. 1, T_i^μ are the targets, *i.e.* the real values of data to be reconstructed/forecast by the NN, O_i^μ are the outputs, *i.e.* the results of the NN in reconstructing/forecasting the targets, h_j^μ and h_i^μ are the weighted sums converging to the neurons of the hidden and output layers, respectively, g_j and g_i are the sigmoids calculated at hidden and output neurons, V_j^μ represent what exits from the hidden neurons after the calculation of their nonlinear transfer functions, g' are the sigmoid derivatives, η is the learning rate, directly associated with the minimization of the total error (a quadratic cost function of T_i^μ and O_i^μ) on the training set *via* gradient descent, and the m-term is the so-called momentum term, useful for avoiding large oscillations in the learning process. A good combination of η and m permits to escape from relative minima of the cost function and to reach a deeper minimum.

Once fixed the weights at the end of the iterative training (on a training set), the network is nothing but a function that maps input values to output ones. If this map shows its validity also for data which are unknown to the network (*i.e.* on validation/test sets), we have found a fully nonlinear regressive law linking input and output data. Of course, methods are to be used in order to prevent overfitting: here, early stopping is adopted.

Together with these quite common features of NN models (see, for instance, refs. [15, 16] for two standard references on these topics), this tool provides also many training/validation/test procedures and facilities which are very useful for handling historical data from complex systems.

3. – Unforced and forced Lorenz systems

In a previous paper [2] an extended and unifying formalism for a class of low-dimensional models, including Lorenz and Kolmogorov ones, has been developed. Here, I deal just with a little generalisation of the Lorenz system, by considering a constant forcing added to each of its equations.

Thus, a general forced Lorenz system reads as follows:

$$\begin{cases} \frac{\mathrm{d}x}{\mathrm{d}t} = \sigma(y - x) + f_x, \\ \frac{\mathrm{d}y}{\mathrm{d}t} = rx - y - xz + f_y, \\ \frac{\mathrm{d}z}{\mathrm{d}t} = xy - bz + f_z. \end{cases} \tag{3}$$

In this paper the choice of the parameters is the same as in [1], *i.e.* $\sigma = 10$, $b = 8/3$ and $r = 28$, so that we recognize the classical chaotic behaviour when $f = 0$. Furthermore, Mittal *et al.* [17] showed that if we consider $f_z = 0$, this is equivalent to shift the parameter r. Thus, we may retain just the forcings in the first two equations of the system (3), without loss of generality.

Therefore, also following the formalism by Palmer [5], we re-write a forced Lorenz system as follows:

$$\begin{cases} \frac{\mathrm{d}x}{\mathrm{d}t} = \sigma(y - x) + f_0 \cos\theta, \\ \frac{\mathrm{d}y}{\mathrm{d}t} = rx - y - xz + f_0 \sin\theta, \\ \frac{\mathrm{d}z}{\mathrm{d}t} = xy - bz. \end{cases} \tag{4}$$

This system has been recently considered by Palmer and co-workers [5,6] in connection with studies about changes in atmospheric regimes induced by external forcings. In particular, they showed that the observed climate change of the last decades "can be interpreted in terms of changes in the frequency of occurrence of natural atmospheric circulation regimes" [6]. In this framework, the Lorenz system (with its wings-regimes) represents a toy model in which we can recover a similar behaviour, if it is forced by a weak external forcing. From this viewpoint that forcing can be interpreted as the analogue of the increase of anthropogenic forcings in the real climate system. A further research showed that a weak forcing added to the original unforced Lorenz model can lead to a relevant increase in the frequency of occurrence of extremely persistent events [18].

In this paper, the system (4) is considered and the case $\theta = 90°$ is explored for several values of f_0. The numerical integration of the system is performed through a 4th-order Runge-Kutta scheme with time step $\Delta t = 0.01$.

A complete mathematical description of the behaviour of a forced Lorenz system is beyond the scope of this paper: more information can be found in [5,17,19]. Here, I report just some qualitative and quantitative considerations useful for the further development of the paper itself.

In fig. 2 the projections of the unforced and a forced Lorenz attractor onto the (x, y)-plane are shown. It is clear that the shapes of the attractors are almost undistinguishable, but, while in the classical unforced case (a) the wings-regimes are equally "visited" (in frequency) by the states of the system, in the forced case (b) the forcing leads to increase the frequency of occurrence of the regime which lies in the positive x-y quadrant.

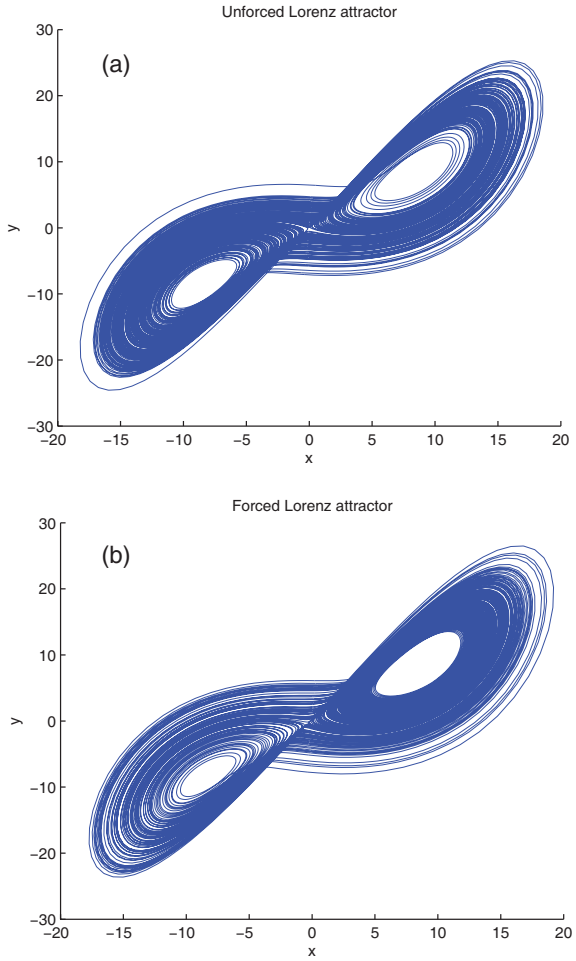

Fig. 2. – Projections onto the (x, y)-plane of both the classical unforced Lorenz attractor (a) and the forced Lorenz attractor with $f_0 = 5$ and $\theta = 90^\circ$ (b).

TABLE I. – *Dynamical variables for the classical unforced Lorenz system ($f_0 = 0$) and for several forced Lorenz systems with $\theta = 90^\circ$ (f. p. means that when $f_0 > 10$ the attractor is a fixed point whose coordinates depend on the intensity of f_0).*

Variable	$f_0 = 0$	$f_0 = 2.5$	$f_0 = 5$	$f_0 > 10$
$\bar{x}$	-0.0476	1.1838	2.7596	f. p.
$\bar{y}$	-0.0473	1.1845	2.7608	f. p.
$\bar{z}$	23.526	23.643	24.029	f. p.
PLE	0.905	0.880	0.759	< 0
DIM	2.062	2.060	2.053	0
$\bar{g}$	9.06×10^{-3}	8.90×10^{-3}	7.56×10^{-3}	< 0

Of course, a rigorous investigation of this phenomenon can be performed if the probability density function of the states associated with the two wings-regimes is calculated, as in Palmer's study [5]. Here, I simply quantify this effect by calculating the mean values $\bar{x}$, $\bar{y}$ and $\bar{z}$ (shown in table I for several values of f_0): one can appreciate a net bias towards the positive x-y quadrant which presents a quasi-linear proportionality to the strength of the forcing.

Apart from the bias just discussed, other dynamical properties of the Lorenz attractor reveal little changes when forcing increases, at least till $f_0 = 5$: this value is considered a limit beyond which the model behaviour changes qualitatively (see, for instance, ref. [19]), finally reaching the situation of a stable fixed point as attractor. In table I the values of the positive Lyapunov exponent (PLE) and of the fractal dimension of the attractor (DIM) are shown (refer to [20,21] for methods of calculation). As well known, their values represent two "measures" of chaos. Note that the differences between the unforced values and the forced ones of PLE and DIM are very little when $f_0 = 2.5$ is considered, while they are quite significant when the forcing is doubled.

4. – Dynamical estimation of predictability

Once summarised the dynamical properties of unforced and forced Lorenz systems in the previous section, let us come to the topic of predictability.

The local predictability on the unforced Lorenz attractor has been extensively studied in [7] by means of the so-called bred-vector growth, *i.e.* the rate of divergence of trajectories starting from very close points on the attractor itself.

A bred vector is a vector $\delta\mathbf{v}$ which simply represents the 3D-Euclidean distance between two states (points) on the Lorenz attractor after a certain number (n) of time steps in two model runs, if the second run is originated from a slight perturbation ($\delta\mathbf{v}_0$) in the initial conditions. We define the bred-growth rate g as

$$g = \frac{1}{n} \ln \left(\frac{|\delta\mathbf{v}|}{|\delta\mathbf{v}_0|} \right). \tag{5}$$

As shown in [7], g can be used to identify regions of distinct predictability on the unforced Lorenz attractor. Furthermore, these authors were able to find prediction rules for regime changes and persistence in a new regime.

Notably, these prediction rules have been reconsidered and improved by Yadav *et al.* [22], who extended their investigation to forced Lorenz models, too. However, if we exclude this particular discovery, no attempt at estimating global or local predictability on forced Lorenz models has been performed, to my knowledge.

Here, by adopting the method by Evans *et al.* [7], after having fixed $n = 8$, a total of 60000 bred-growth rates have been calculated, 20000 related to points of the unforced attractor and the others related to states of two forced attractors with $f_0 = 2.5$ and $f_0 = 5$, respectively. The results for the mean values of g are presented in table I, while in fig. 3 two plots of growth-rate classes on the unforced and a forced attractor are shown. In table II the notation adopted for the specific division into predictability classes is explained.

A quick look at fig. 3 leads to appreciate that regions of distinct predictability exist on the attractors: anyway, the two pictures (a and b) are quite similar and we are not able to distinguish clear changes in the local predictability distributions.

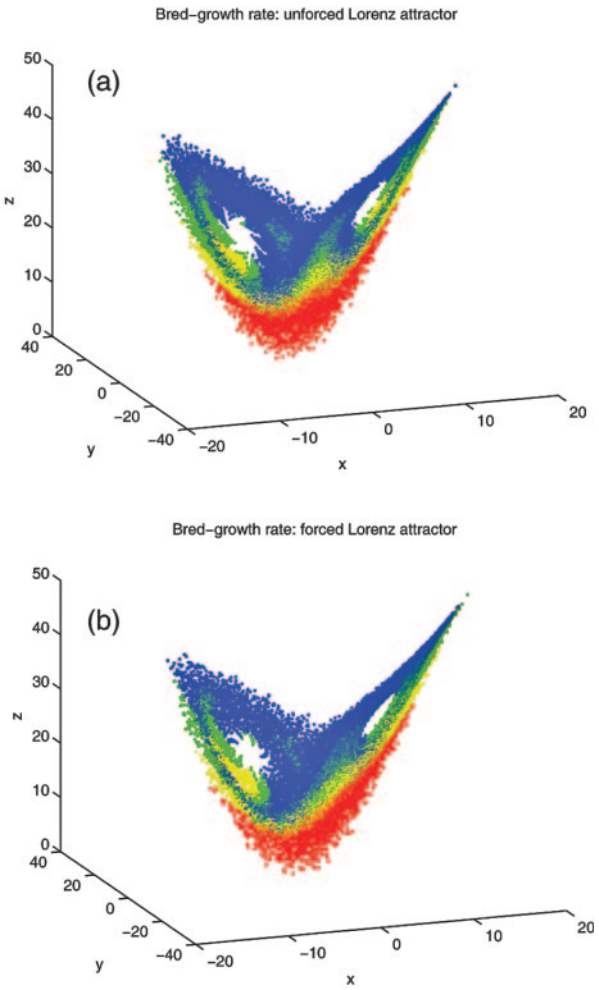

Fig. 3. – Regions of distinct local predictabilities on the unforced Lorenz attractor (a) and on a forced one with $f_0 = 5$ and $\theta = 90^\circ$ (b).

TABLE II. – *The predictability classes considered in this paper.*

Class	Bred-growth rate
Blue	$g < 0$
Green	$0 \leq g < 0.04$
Yellow	$0.04 \leq g < 0.064$
Red	$g \geq 0.064$

TABLE III. – *Number of states belonging to each class of predictability on the unforced Lorenz attractor and on two forced ones.*

Class	$f_0 = 0$	$f_0 = 2.5$	$f_0 = 5$
Blue	10185	10270 (+0.8%)	10535 (+3.4%)
Green	4469	4475 (+0.1%)	4488 (+0.4%)
Yellow	2569	2526 (−1.6%)	2601 (+1.3%)
Red	2777	2729 (−1.8%)	2376 (−14.4%)

On the other hand, an analysis of the mean values of g ($\bar{g}$) in table I shows that a sensible (nonlinear) decrease in the bred-growth rate happens when the forcing achieves $f_0 = 5$. Some more piece of information is given in table III, where the number of states associated with a certain class of g is shown: clearly, one is able to appreciate a consistent increase in the blue class and an even more significant decrease in the red class when passing from the unforced situation to the forced one with $f_0 = 5$. In short, a clear increase in predictability is shown in the stronger forced situation.

As a consequence of this brief dynamical analysis, in what follows I will limit to compare results between the unforced situation and the case $f_0 = 5$: this value of the external forcing is enough for obtaining consistent dynamical differences but does not change the general (chaotic) behaviour of the model.

5. – Neural network estimation of predictability

Applying NNs to the study of the Lorenz system (in particular, forecasting its future states) is not a new idea. Nevertheless, past attempts essentially dealt with the prediction of the time series for a single variable of the Lorenz system (usually the x variable), with the aim of reconstructing its complete dynamics under the conditions prescribed by the Takens theorem [23]: see, for instance, [24, 25] and references therein. This permits to mimic the reconstruction of an unknown dynamics by observational data in a complex system.

Furthermore, a notable paper, which is related to the rules cited at the previous section about regime changes, is that by Roebber and Tsonis [26], where the authors used NNs as a method to improve the prediction of flow transitions in the cases of two simple mathematical systems.

In the present paper, instead, my fundamental aim is to assess if NNs are able to supply an "operational" estimation of predictability on unforced and forced Lorenz attractors. In order to achieve this final goal, two preliminary tests shall be performed, just to verify that the NN forecasting performance is sensitive to different local predictabilities and to their changes in forced situations.

Therefore, once considered the full dynamics of the unforced and forced Lorenz systems, a first attempt at forecasting the final states after n integrations steps is performed by means of networks endowed with 3 inputs (the initial 3D-coordinates), 15 neurons in a hidden layer and 3 outputs (the final 3D-coordinates). Here I do not discuss how to choose the optimal topology for networks. It is worthwhile to note that 15 neurons in a unique hidden layer are sufficient to obtain a good representation of the underlying

TABLE IV. – *Performance of NN forecasts on the test sets in terms of mean distance between output and target points.*

Class	$f_0 = 0$	$f_0 = 5$
Blue	5.66 ± 0.15	5.24 ± 0.23
Green	6.58 ± 0.25	6.14 ± 0.20
Yellow	6.62 ± 0.24	6.11 ± 0.30
Red	8.36 ± 0.41	8.30 ± 0.45

function but not so many to determine some kind of overfitting. Furthermore, I would like to stress that, in what follows, the attention will be paid more on the possibility of achieving certain results by NN modelling than on the rate of performance obtained by the specific model adopted. As we will see in the final section, increase in performance can be envisaged by use of different input variables and/or different NN models.

For each class of bred-growth rate, the NN model is trained to make a single-step forecast from t_0 to $t_0 + n$ (here, of course, $n = 8$ is chosen, as in the bred-growth calculations). Attempts at performing 8 forecast steps (to achieve the same final forecast horizon) result in very poor performance, as already noted in other studies [13] and as known from theoretical considerations [27]. The total sets of Lorenz simulated data (20000 input-target patterns for each case) are divided into a training set (60% of data), a validation set (20%) and a test set (20%). The 3 outputs represent the forecast 3D-position after 8 time steps of dynamical integration. Here the 3D-Euclidean distance between output and target points is considered as a measure of forecasting performance: of course, lower is this distance better is the performance of the NN model.

As shown in table IV, the results of the NN model in the forecasting activity (expressed in terms of the mean distance between output and target points) clearly depend on the bred-growth classes and exhibit the best performance on the blue region of the attractors and the worst one on the red points (in both unforced and forced cases). Performance on green and yellow classes presents intermediate values and, even if it is impossible to distinguish between them because each value falls inside the error bar associated to the other one, however these are well separated from the performance values of the other two classes (blue and red). These error bars are deduced from results of ensemble runs of the NN model starting from distinct random values of initial weights, so that the networks are able to widely explore the landscape of the cost function. In table IV the error bars represent ± 2 standard deviations.

In particular, referring to the forced system, one find that, analogously to the decrease of the mean value of g in table I, also the total mean forecast error of the NN model decreases. This is an expected result, because now there is a net shift of less predictable points to more predictable ones (see table III), with a more frequent permanence of the system's state in regions of high predictability. Furthermore, the results on the blue region show a statistical significant improvement in performance in this specific class and also the improvements in green and yellow class are close to a full statistical significance: this could suggest that changes in predictability, locally on the attractor, can be important, even if this hypothesis is not verifiable in this context.

In short, the goodness of a NN forecast is related to the specific class of predictability. Moreover, we can appreciate a net increase in both dynamical predictability and NN performance in a forced situation.

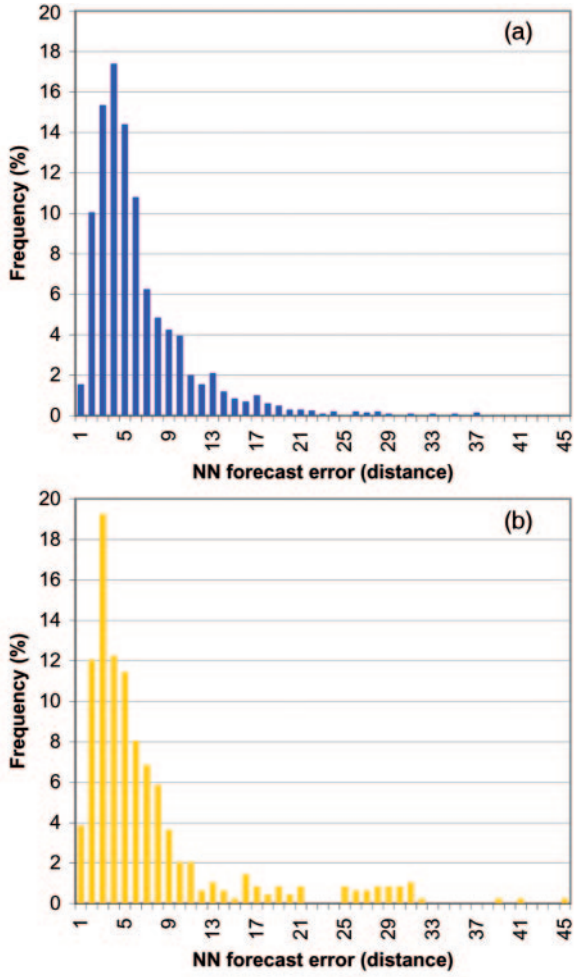

Fig. 4. – Error distribution in NN forecasts for the blue class (a) and the yellow class (b) on the unforced Lorenz attractor.

A closer look at these results, in terms of the distributions of NN forecast errors for each class, permits to reveal that unimodal distributions (for blue and green classes) tend to split to quasi-bimodal distributions for yellow and red classes. In fig. 4a,b these distributions are shown for the blue and the yellow class, respectively, in the unforced case. Similar results hold for NN modelling on the forced systems. This fact implies a sensitivity of forecast performance to regions where a change of regime is possible and two close trajectories could evolve to opposite wings on the attractor. For instance, if one refers to fig. 3, it is very clear that the trajectories which end onto red points come from the middle of the attractor where they undergo a "split" towards the left or the right wing of the attractor itself.

Now, once recognised the sensitivity of NN forecast performance to different regions of predictability and the increase in predictability (and NN performance) when a weak forcing is superimposed to the classical Lorenz system, one can ask how to use these properties for an operational estimation of the predictability of a single Lorenz state.

TABLE V. – *Performance of NN estimation of the bred-growth rates on the test sets in terms of the linear correlation coefficient (NN forecasts vs. calculated values through dynamical integration). The error bars represent ±2 standard deviations.*

	$f_0 = 0$	$f_0 = 5$
R	0.660 ± 0.011	0.684 ± 0.010

In this framework, it is worthwhile to stress that the consideration of NN forecasting performance represents just an *a posteriori* recognition of the predictability of a state on the Lorenz attractors. In fact it is available only after our knowledge of the results of the dynamical integration of the Lorenz system, while, from an operational point of view, the single NN forecasts give us just information about a possible trajectory, with no relation to predictability.

As a matter of fact, in table IV the increase in the amplitude of error bars in NN performance when going from low bred-growth rates to high ones is clearly visible. Therefore, this can lead to explore a NN ensemble forecast approach by supposing that the spread of NN ensemble forecasts on distinct points could resemble a similar increase and could become an index of the particular local predictability of any Lorenz state. Unfortunately, the not very good NN forecasting performance (to be briefly discussed later) does not permit to find significant results by this attempt.

Therefore, in this paper a different approach is followed: a NN forecast of bred-growth rates for any point of the attractors is performed, leading us to obtain a direct estimation of this variable, which well represents the local predictability values. In doing so, NNs endowed with 3 inputs, 30 neurons in a hidden layer and 1 output are used.

As shown in table V, even if the networks adopted here are very simple, the NN forecasts of bred-growth rate show quite good performance and contribute to open a new scenario in which NNs could be operationally used for estimations of the local predictability referred to single states on the Lorenz attractors. Furthermore, a statistical significant increase in performance is shown when an external forcing is applied. This reveals that, not only the presence of an external forcing permits to better forecast the future states on the attractors (as already shown), but also the estimation of predictability itself by NNs is always possible and it is improved in forced situations: the latter are independent and new results.

In order to obtain some more piece of information on the ability of the NN model to recognise different classes of predictability, a simple statistical analysis can be performed by means of a contingency table (table VI), where the threshold for bred-growth rate is fixed to 0.04: this value allows us to understand how well NNs can discern about

TABLE VI. – *Contingency table at a defined threshold distinguishing between events and non-events.*

DET \ FOR	No	Yes	Sum
No	a	b	g
Yes	c	d	h
Sum	e	f	n

TABLE VII. – *Indices of performance in NN forecasts of the bred-growth rate (threshold* $= 0.04$*).*

Index	$f_0 = 0$	$f_0 = 5$
POD	0.907	0.941
FAR	0.154	0.138
HR	0.810	0.841
CSI	0.778	0.818
HSS	0.289	0.512

situations in which trajectories may be undergone to "splits" or not (see the discussions above).

Referring to table VI, several indices of performance are calculated as follows for two runs of the NN model:

POD (Probability Of Detection) $= d/h$;

FAR (False Alarm Ratio) $= b/f$;

HR (Hit Rate) $= (a + d)/n$;

CSI (Critical Success Index) $= d/(b + h)$;

HSS (Heidke's Skill Statistics) $= [2(ad - bc)]/(gf + he)$.

The results are shown in table VII. As one can see, the forecasting performance in estimating local predictability is always better in the forced situation. Because of the goodness of HSS as a measure of performance (see, for instance, the discussion in [28]), the big difference in its values appears as particularly significant.

6. – Conclusions and prospects

In this paper a non-dynamical approach (NN modelling) has been applied to the analysis of predictability in unforced and forced Lorenz systems.

First of all, the evidence of increased predictability in forced situations has been obtained by a dynamical method. Then, the application of NN modelling led to further results:

– the performance of NNs in forecasting future states on the Lorenz attractors depends on the predictability class of the states themselves. In this framework, when passing from the unforced Lorenz system to a forced one, predictability increases and, analogously, NN performance increases as well. This preliminary result shows the sensitivity of NN forecasting to the values of local predictability and leads to rediscover an increase of predictability in forced situations also by a non-dynamical method: the NN forecasting performance. However, it does not permit to obtain an operational estimation of the predictability itself.

– This operational estimation has been achieved by directly forecasting the values of bred-growth rate *via* NNs. In this context, after having seen that the presence of a weak external forcing leads to better forecasting the future states of the system,

now we recognise that even local predictability is operationally better forecasted in a forced situation.

As far as further possible consequences of the present work are concerned, it is worthwhile to stress what follows:

– if we adopt a Palmer framework [5, 6], in which Lorenz systems are seen as toy models of the climate and its atmospheric subsystem, the present paper leads to envisage an increased predictability in future meteo-climatic scenarios characterised by increased anthropogenic forcings;

– the operational forecast of predictability by NN modelling leads to envisage the possibility to emulate the ensemble forecasts obtained through (very time-consuming) dynamical integrations, by evaluating the predictability of single meteorological states in realistic models by NNs.

But, before going to more realistic applications, further development is needed in the framework of toy models. For instance, as cited above, the NN performance is not very good in the results described in sect. **5**. This can be due to the limited length of the record containing input-target pairs for training and validation, to the very preliminary structure of the input patterns themselves and to the simple architecture and training rules of the NNs used in this study.

Thus, possible developments of this work concern the building of an extended data set by prolonged Runge-Kutta integrations, the insertion of different inputs (for instance a truncated time series of delayed data) and the application of other NN architectures (such as recurrent NNs) and training rules.

* * *

M. Peña and E. Kalnay are kindly acknowledged for having allowed me to use their code in the calculation of bred vectors.

REFERENCES

[1] Lorenz E. N., *J. Atmos. Sci.*, **20** (1963) 130.
[2] Pasini A. and Pelino V., *Phys. Lett. A*, **275** (2000) 435.
[3] Gedalin M. and Balikhin M., *Nonlinear Processing Geophys.*, **15** (2008) 541.
[4] Palmer T. N., *Weather*, **48** (1993) 313.
[5] Palmer T. N., *J. Clim.*, **12** (1999) 575.
[6] Corti S., Molteni F. and Palmer T. N., *Nature*, **398** (1999) 799.
[7] Evans E., Bhatti N., Kinney J., Pann L., Peña M., Yang S.-C., Kalnay E. and Hansen J., *Bull. Am. Meteorol. Soc.*, **85** (2004) 520.
[8] Pasini A., in *Artificial Intelligence Methods in the Environmental Sciences*, edited by Haupt S. E., Pasini A. and Marzban C. (Springer, Berlin) 2009, pp. 235-254.
[9] Krasnopolsky V. M., Fox-Rabinovitz M. S. and Belochitski A. A., *Mon. Weather Rev.*, **136** (2008) 3683.
[10] Pasini A. and Potestà S., *Nuovo Cimento C*, **18** (1995) 505.
[11] Pasini A., Pelino V. and Potestà S., *J. Geophys. Res.*, **106** (D14) (2001) 14951.
[12] Pasini A., Perrino C. and Žujić A., *Nuovo Cimento C*, **26** (2003) 633.
[13] Pasini A. and Ameli F., *Geophys. Res. Lett.*, **30** (2003) 1386, doi:10.1029/2002GL016726.
[14] Pasini A., Lorè M. and Ameli F., *Ecol. Modell.*, **191** (2006) 58.
[15] Hertz J., Krogh A. and Palmer R. G., *Introduction to the Theory of Neural Computation* (Addison-Wesley, New York) 1991.

[16] Bishop C. M., *Neural Networks for Pattern Recognition* (Oxford University Press, Oxford) 1995.
[17] Mittal A. K., Dwivedi S. and Pandey A. C., *Nonlinear Processing Geophys.*, **12** (2005) 707.
[18] Khatiwala S., Shaw B. E. and Cane M. A., *Geophys. Res. Lett.*, **28** (2001) 2633.
[19] Annan J. D., *Tellus A*, **57** (2005) 709.
[20] Wolf A., Swift J. B., Swinney H. L. and Vastano J. A., *Physica D*, **16** (1985) 285.
[21] Briggs K., *Phys. Lett. A*, **151** (1990) 27.
[22] Yadav R. S., Dwivedi S. and Mittal A. K., *J. Atmos. Sci.*, **62** (2005) 2316.
[23] Takens F., in *Dynamical systems and turbulence*, edited by Rand D. A. and Young L.-S., *Lecture Notes in Mathematics*, Vol. **898** (Springer, Berlin) 1981, pp. 366-381.
[24] de Oliveira K. A., Vannucci A. and da Silva E. C., *Physica A*, **284** (2000) 393.
[25] Boudjema G. and Cazelles B., *Chaos, Solitons Fractals*, **12** (2001) 2051.
[26] Roebber P. J. and Tsonis A. A., *J. Atmos. Sci.*, **62** (2005) 3818.
[27] Atiya A. F., El-Shoura S. M., Shaheen S. I. and El-Sherif M. S., *IEEE Trans. Neural Netw.*, **10** (1999) 402.
[28] Marzban C., *Weather For.*, **13** (1998) 753.